Analysis and Investigation of Direct AC-AC Quasi – Resonant Converter

Mihail Hristov Antchev

Department of Power electronics, Technical university-Sofia, Sofia, Bulgaria

**Email address:**

antchev@tu-sofia.bg

Abstract: The present article reports an analysis and investigation of direct AC-AC quasi-resonant converter. A bidirectional power device, whose switching frequency is lower than the frequency of the current passing through the load, is used for its realisation. A mathematical analysis of the processes has been made and comparative results from computer simulation and experimental study have been brought. The converter can find application in wide areas of power electronics: induction heating, wireless power transfer, AC-DC converters.

Keywords: Quasi – Resonant Converter, Constant Frequency

1. Introduction

The standard method of converting AC to AC power is by rectifier, supplying power to inverter, to whose output is connected the load. The so called "direct converters" are used to increase the energy efficiency. There are matrix converters for direct AC to AC power conversion [1,2]. Resonant converters are also used for the same purpose [3,4,5]. In [6] a direct AC-AC resonant converter has been considered, using two bidirectional power devices, including an active-inductive load while switching to the power supply. The converter described in [7,8] uses 4 power devices, and during the active intervals a serial oscillator circuit is connected to the input voltage source. The converter presented in [9] uses two bidirectional power devices, an additional capacitor for soft switching and a serial oscillator circuit connected to the input voltage at specified intervals. The induction heating converter described in [10] is most similar to the converter presented in this paper. An analysis has been made on the assumption that the converter is supplied with DC voltage, whose value is equal to the effective value of the AC input voltage, which does not correspond to the actual physical action. The "multi-cycle modulation" used in the study provides only discrete power regulation of the load and the use of variable switching frequency deteriorates the electromagnetic compatibility.
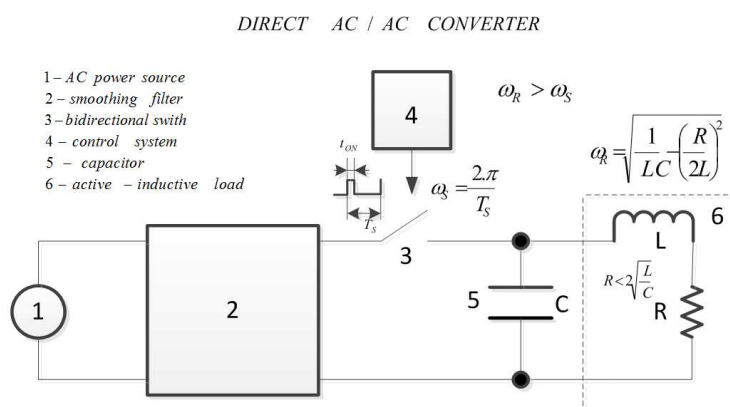
Figure 1. Block diagram of the new AC-AC quasi-resonant converter.

The purpose of the present paper is to give more accurate mathematical analysis, suitable for testing the converter's operation in random mode, and not only in the so called "multi-cycle modulation", which is a particular case of the present investigation. Constant frequency and pulse width modulation operation is proposed for the power regulation.

Fig.1. shows a block diagram to illustrate the implementation of the considered converter.

Its effect is similar to that of the so called "class E-inverters" [11,12]. When switching on the bidirectional switch 3 for time t_{ON} the capacitor 5 is quickly charged to the momentary value of the AC input voltage. This voltage is applied also to the load 6 and the current passing through it increases in absolute value. When turning off the switch for time $T_S - t_{ON}$, damped oscillations develop in the oscillator circuit, composed of load and capacitor, with frequency ω_0, determined by the elements values. The process of switching is repeated at a period $T_S > T_0$, and each switching on in the circuit adds energy. This energy can be regulated via change in time t_{ON} at constant switching frequency ω_S. This frequency is much bigger than the frequency of the source 1 AC input voltage. With the help of the smoothing filter 2 the higher harmonics of the switch current are removed. Thus the current from the AC voltage source has an almost sinusoidal shape.

2. Mathematical Description

Fig.2 shows the implemented power circuit, which will be used also for mathematical analysis. The timing diagrams of the basic values are shown on fig.3 for one switching period T_S. The analysis in one switching period is divided in two intervals: the first with duration t_{ON}, and the second - $T_S - t_{ON}$. The aim is to obtain expressions for the basic values during both intervals: the current through the inductance, capacitor's voltage and the current through the bidirectional switch.

For the first interval with duration t_{ON} the current through the load inductance changes from I_{t_0} to I_{LtON}. The value of the capacitor's voltage is constant,
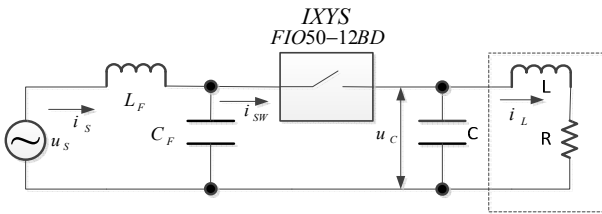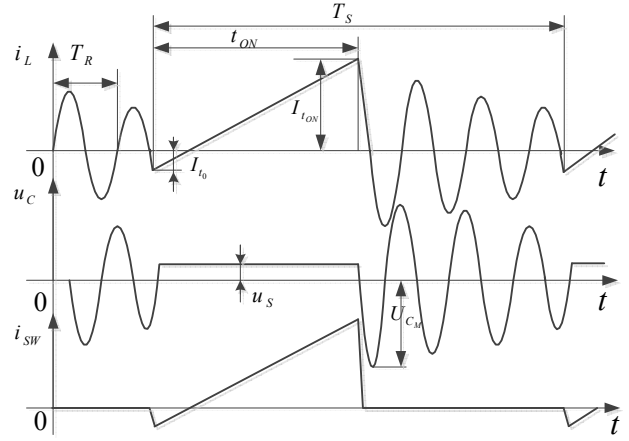
Figure 2. *Practical design of the converter.*

Figure 3. *Waveforms for analysis: top- inductor current i_L, middle-capacitor voltage u_C, bottom – bidirectional switch current i_{SW}.*

equal to the momentary value of the input voltage (due to the high switching frequency of the switch).

$$u_C = u_S \qquad (1)$$

The differential equation has the form

$$u_S = L.\frac{di_L}{dt} + R.i_L \qquad (2)$$

From the initial condition

$$i_L(t = 0) = I_{t_0} \qquad (3)$$

is determined the integration time constant and this gives

$$i_L(t) = \frac{u_S}{R} + \left(I_{t_0} - \frac{u_S}{R}\right).e^{-\frac{t}{\tau}}, \qquad (4)$$

where $\tau = \frac{L}{R}$.

The current value at the end of the interval is:

$$i_L(t_{ON}) = I_{LtON} = \frac{u_S}{R} + \left(I_{t_0} - \frac{u_S}{R}\right).e^{-\frac{t_{ON}}{\tau}} \qquad (5)$$

The average current value through the switch is determined by:

$$I_{SW_{AVR}} = \frac{1}{T_S}\int_0^{t_{ON}} i_L(t).dt \ , \qquad (6)$$

where substitution of (4) and transformation leads to the following result:

$$I_{SW_{AVR}} = \frac{u_S}{R}.\frac{t_{ON}}{T_S} + \frac{\tau}{T_S}.\left(I_{t_0} - \frac{u_S}{R}\right).\left(1 - e^{-\frac{t_{ON}}{\tau}}\right) \qquad (7)$$

For the second interval with duration $T_S - t_{ON}$ the current changes from I_{LtON} to I_{t_0}. The last value is used as initial in the next switching period. The differential equation has the form:

$$L.\frac{di_L}{dt} + R.i_L + \frac{1}{C}\int i_L.dt = 0 \qquad (8)$$

The solution is:

$$i_L(t) = e^{-\delta t}.\left(C1.\cos\sqrt{\omega_R^2 - \delta^2}.t + C2.\sin\sqrt{\omega_R^2 - \delta^2}.t\right), \quad (9)$$

where $\delta = \frac{R}{2L}; \omega_R = \frac{1}{LC}$

$$\text{Accepting that } \omega_0 = \sqrt{\omega_R^2 - \delta^2} \qquad (10)$$

$$i_L(t) = e^{-\delta t}.(C1.\cos\omega_0 t + C2.\sin\omega_0 t) \quad (11)$$

The integration constants are determined by the following conditions:

$$i_L(t = 0) = I_{LtON} \rightarrow C1 = I_{LtON} \qquad (12)$$

$$i_L\left(t \approx \frac{T_R}{4}\right) = 0 \rightarrow C2 = -I_{LtON}.\cot\omega_0.\frac{T_R}{4} \quad (13)$$

The final value of the current in this interval I_{t_o} is obtained using (11) for time $T_S - t_{ON}$.

Through integration is obtained the law on capacitor voltage variation:

$$u_C(t) = \frac{1}{C}\int i_L(t).dt \qquad (14),$$

i.e.

$$u_C(t) = \frac{e^{-\delta t}}{C.\omega_R^2}[(C1.\omega_0 - C2.\delta).\sin\omega_0 t - (C2.\omega_0 + C1.\delta).\cos\omega_0 t] \quad (15)$$

Its maximum value for this switching cycle is:

$$u_C\left(t \approx \frac{T_R}{4}\right) = u_{CM} \rightarrow u_{CM} = \frac{e^{-\delta\frac{T_R}{4}}}{C.\omega_R^2}.\left[(C1.\omega_0 - C2.\delta).\sin\omega_0.\frac{T_R}{4} - (C2.\omega_0 + C1.\delta).\cos\omega_0.\frac{T_R}{4}\right](16)$$

The maximum value of the capacitor's voltage corresponds to the switching cycle around the maximum value of the power supply voltage. The last values of the variables in each interval are used as initial values in the next one. For the first switching period after the input voltage passes through zero $I_{t_0} = 0$. Thus all values can be determined by sequential calculation from the moment the input AC voltage passes through zero to the end of its half-period.

3. Computer Simulation

An investigation has been made of the proposed converter's operation using the PSIM program. Fig.4 shows the circuit for computer simulation. The value of the resonant inductance is $100\mu H$, of the resistor in the oscillator circuit - 0.01Ω. The value of the resonant capacitor is $10nF$. The values of the smoothing input filter elements are: $L_F = 680\mu H, C_F = 20\mu F$. The maximum value of the input voltage is $70V$, and its frequency - $50Hz$. The switching frequency of the switch is set to $10kHz$, changing the time t_{ON}. The results from the simulation at $t_{ON} = 30\mu S$ are shown on fig.5, fig.6 and fig.7 in different time scale, in order to track the operation in one switching cycle, as well as for a longer period.
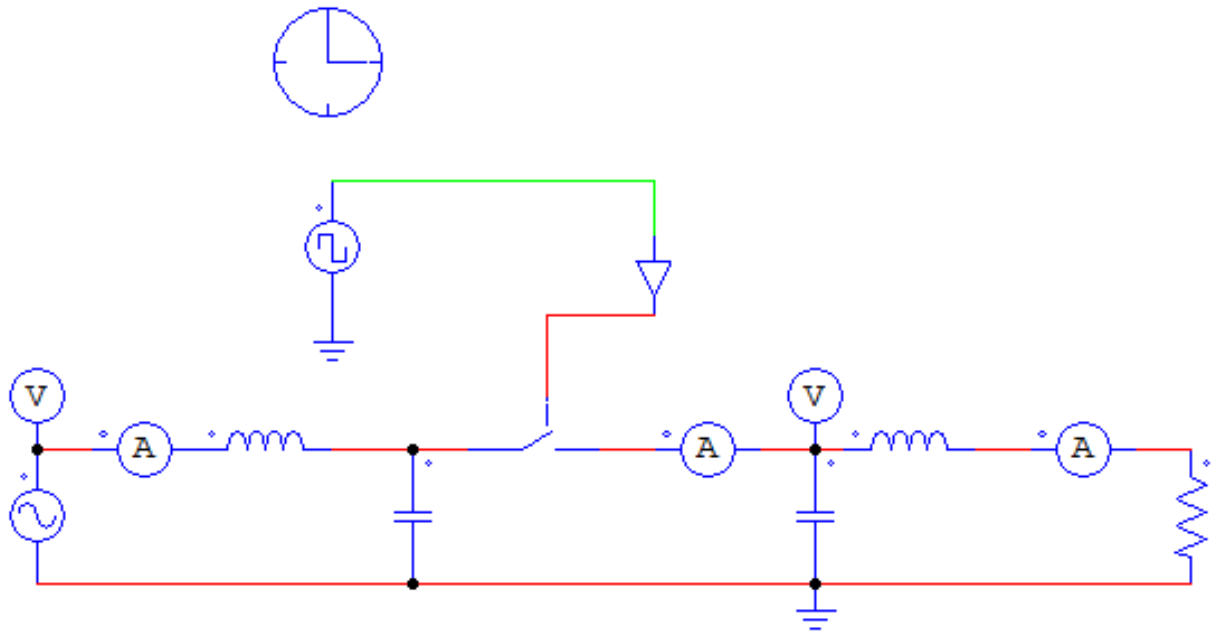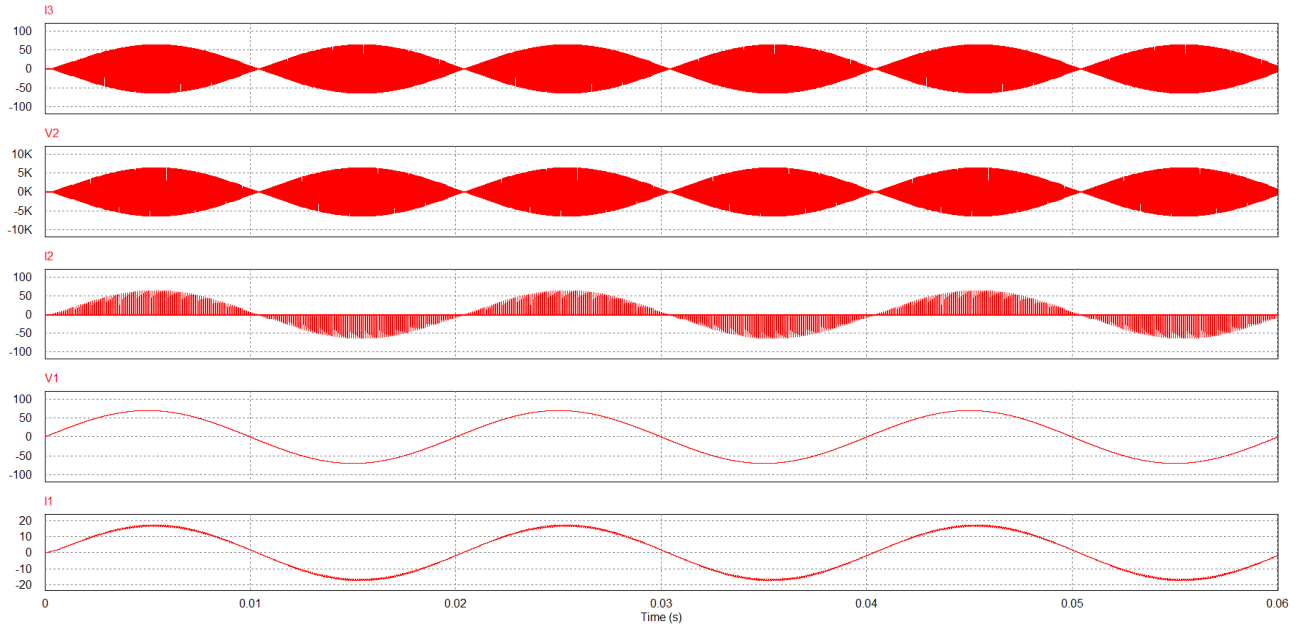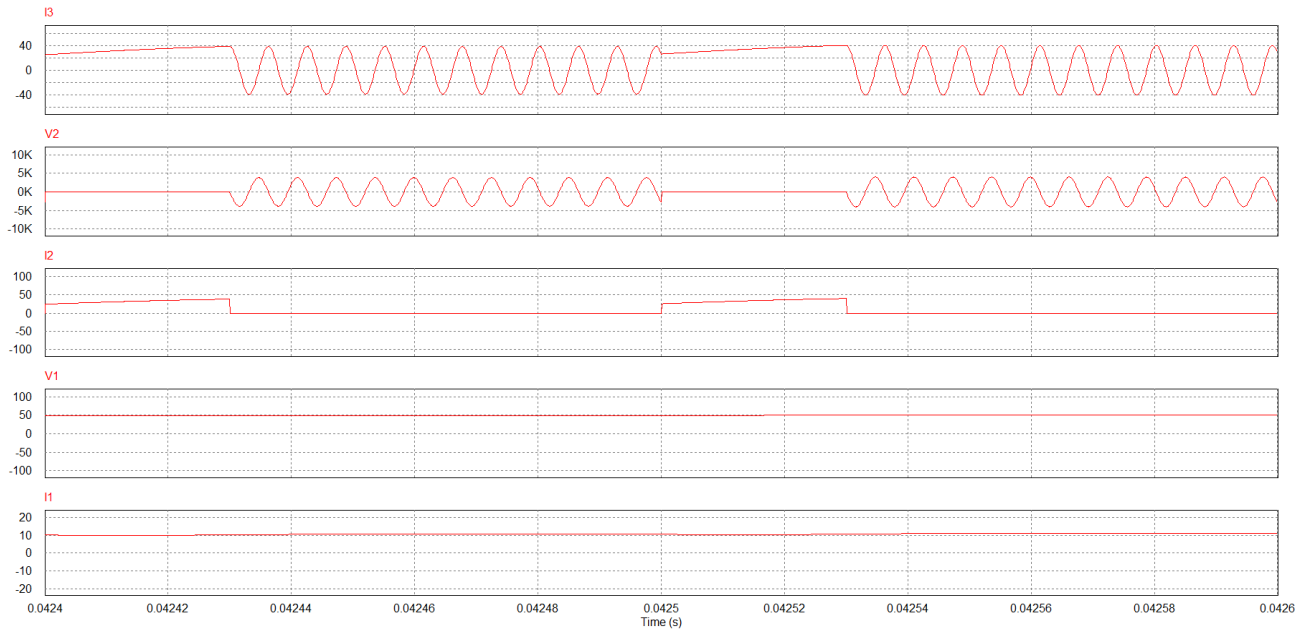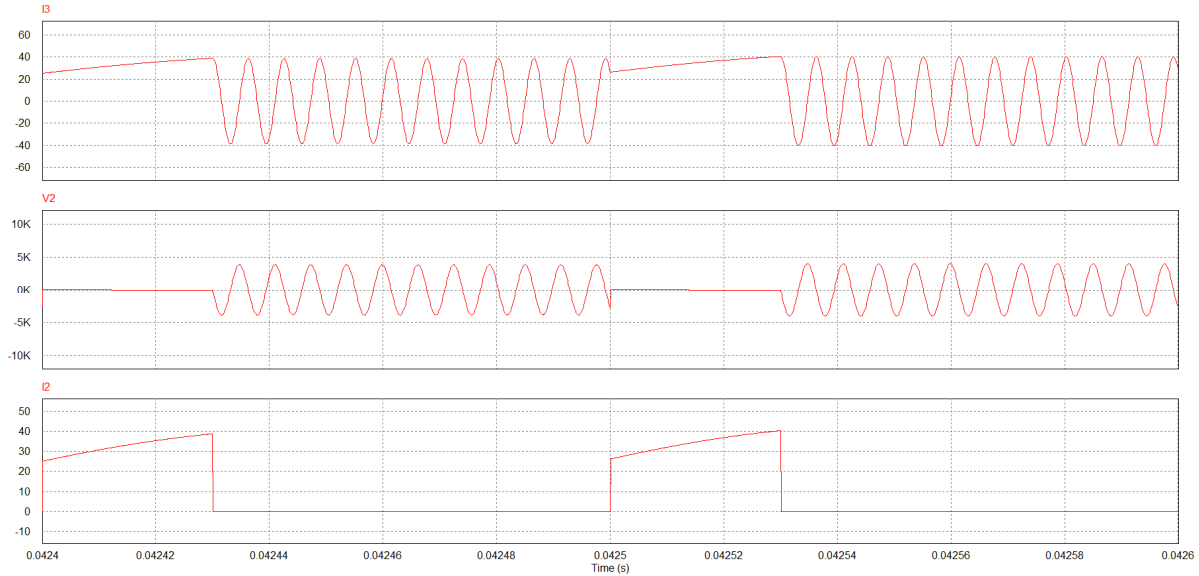

Figure 4. *Circuit for computer simulation.*

Figure 5. *Results from simulation: from top to bottom inductor current i_L, capacitor voltage u_C, bidirectional switch current i_{SW}, input voltage u_S, input current i_S; X-axis – from 0 to 60mS.*

Figure 6. *Results from simulation: from top to bottom inductor current i_L, capacitor voltage u_C, bidirectional switch current i_{SW}, input voltage u_S, input current i_S; X axis – from 42.4 mS to 42.6mS.*

Figure7. *Results from simulation: from top to bottom inductor current* i_L *, capacitor voltage* u_C *, bidirectional switch current* i_{SW} *; X axis – from 42.4 mS to 42.6mS.*
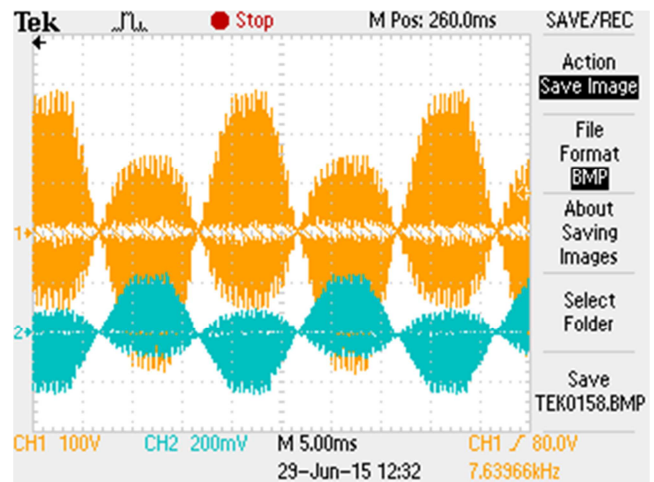
For the cycle shown on fig. 7 a comparison has been made between the results from the computer simulation and those from the calculations according to the mathematical analysis formulas. From fig.7 are taken the readings from the simulation for the current $I_{t_0} = 26.46A$ and the voltage in the beginning of the interval $u_S = 63.1V$. Following formula (5) is calculated $I_{LtON} = 45.31A$, and fig.7 reports a value of $40.28A$. The value obtained from the simulation is smaller, as at the end of the first interval the voltage decreases and the result from fig. 7 reports a value for $u_S = 28.37V$. This decrease accounts for the difference in the average values of the current through the switch – calculated according to (7) $8.03A$, and according to fig.7 with the corresponding PSIM function $10.23A$. The constants $C1 = 40.28$ and $C2 = 0.032$ are calculated using the formulas (12) and (13), and formula (16) is used to obtain the maximum value of the capacitor's voltage $u_{CM} = 4027.56V$. Fig.7 reports a value of $4007V$.

4. Experimental Investigation

An experimental investigation of the converter has been made, carried out according to the scheme shown on fig. 2. The element's values are the same as those from the computer simulation except for the resistor in the oscillator circuit. The measurement shows, that the inductance used in the circuit has a value equal to $100\mu H$ within the range from $5kHz$ to $120kHz$. The value of its resistance from the serial equivalent circuit at $100kHz$ is 1Ω. Therefore the damping in the oscillator circuit will be greater in comparison with that in the computer simulation. The results from the experimental investigation are shown on fig.8, fig.9, fig.10, fig.11, fig.12 and fig.13 in different time scales.
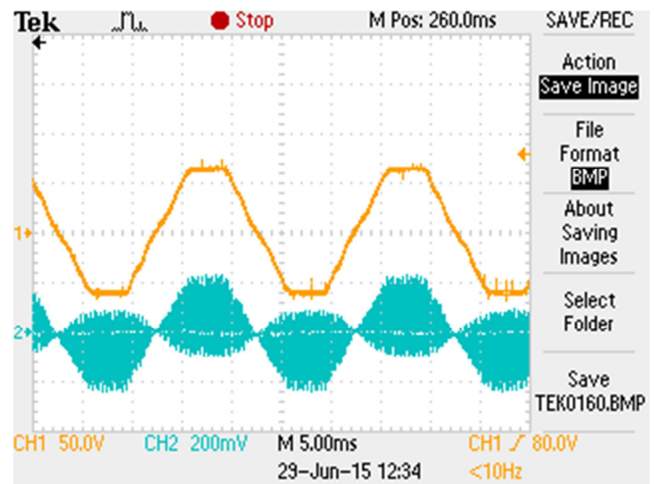
Figure 8. *CH1- input voltage, CH2 – inductor current – 2A/div.*

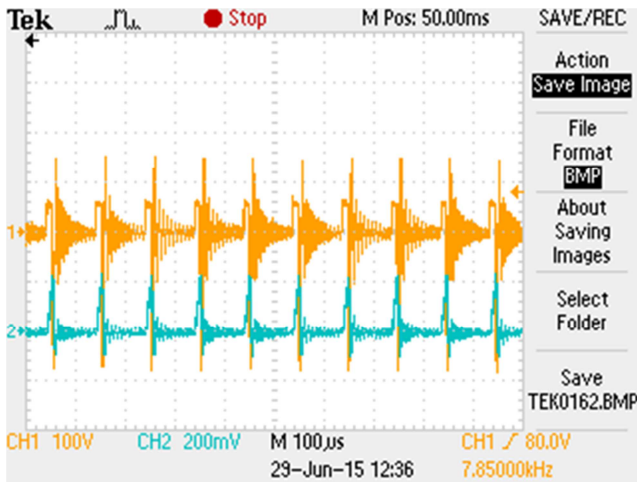***Figure 9.*** *CH1- capacitor voltage, CH2 – inductor current – 2A/div.*

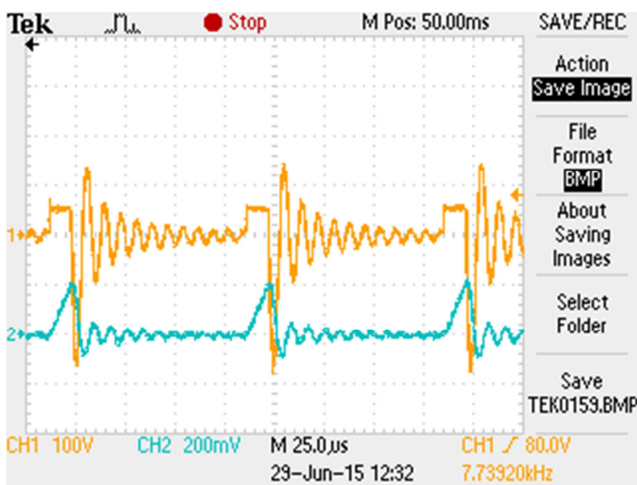*Figure 10.* CH1- capacitor voltage, CH2 – inductor current – 2A/div.

Figure 11. CH1- capacitor voltage, CH2 – inductor current – 2A/div.
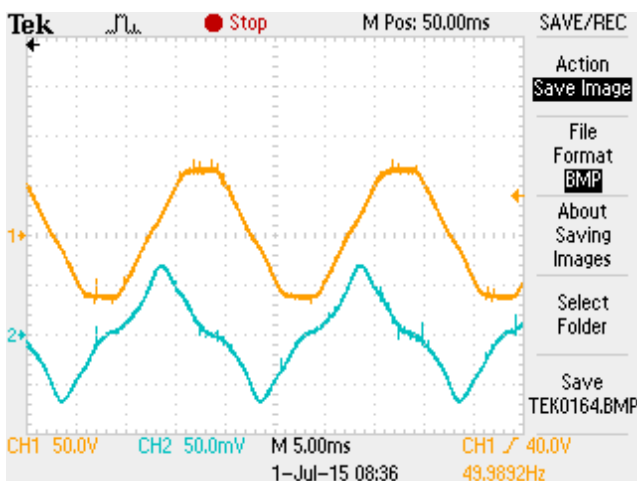

Figure 12. CH1- input voltage, CH2 – input current – 0.5A/div., $t_{ON} = 10\mu S$.
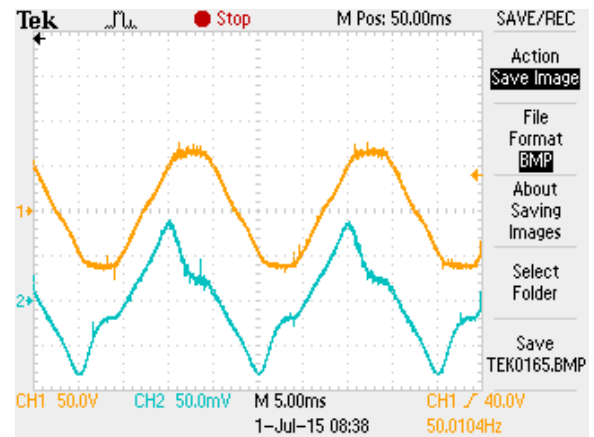

Figure 13. CH1- input voltage, CH2 – input current – 0.5A/div., $t_{ON} = 15\mu S$

A comparison between the results from the experimental investigations and those from the calculations according to the mathematical analysis formulas has been made for the cycle shown on fig. 11. On fig.11 the reported current is $I_{t_0} \approx 0$ and $u_S = 45V$. Using formula (5) is calculated $I_{LtON} = 3.04A$, and from fig.11 the reported value is $2.4A$. Formulas (10) and (11) are used for the calculation of the constants $C1 = 2.4$ and $C2 = 0.0017$, and according to formula (14) is calculated the maximum value of the capacitor's voltage $u_{CM} = 238V$. Fig.11 gives a value equal to $280V$.

Fig.11 shows also that the damping in the experimental circuit is considerably greater than that in the computer simulation. Fig.12 and fig.13 show, that the shape of the current from the source is near to the sinusoidal. The first harmonic current is ahead of the voltage, which can be seen on fig.5. This is due to the greater value of the input filter capacitor. Increasing the switching time of the bidirectional power device reduces the dephasing, and the converter is approaching the active load with respect to the source. A power factor close to 1 could be achieved by appropriate design of the input filter and power device control system synchronisation.

5. Conclusions

The present paper provides a mathematical analysis of a direct AC-AC quasi-resonant converter. The analysis is based on a sequential calculation of the main values in each switching cycle from the beginning to the end of the input AC voltage half cycle. The comparison of the analysis results with those from the computer simulation and the experimental investigations shows good coincidence in the values of the key variables.

References

[1]   Chlebis P., P.Simonik, M.Kabasta, The Comparision of Direct and Indirect Matrix Converters, Progress In Electromagnetics Research Symposium Proceedings Proceedings, Cambridge, USA, July, 2010, pp. 310-313 .

[2] Trentin A., P. Zanchetta, J. Clare, P. Wheeler, Automated Optimal Design of Input Filters for Direct AC/AC Matrix Converters, IEEE Transactions on Industrial Electronics, Vol.59, No.7, July 2012, pp.2811-2822.

[3] Bland M., L.Emprinham , J.Clare, P.Wheeler, A New Resonant Soft Switching Topology for Direct Ac-AC Converters, Power Electronics Specialist Conference proceedings, 2002, pp.72-77.

[4] Sornago H., O. Lucia, A. Mediano, J. Burdio, Direct AC-AC Resonant Boost Converter for Efficient Domestic Induction heating Application, IEEE Transactions on Power Electronics, Vol.29, No.3, March 2014, pp.1128-1140

[5] Sornago H., O. Lucia, A. Mediano, J. Burdio, Efficient and Cost – Effective ZCS Direct AC-AC Resonant Converter for Induction Heating , IEEE Transactions on Industrial Electronics, Vol.61, No.5, May 2014, pp.2546-2556.

[6] Moghe R., R.P.Kandula, A.Iyer, D.Divan, Losse in Medium – Voltage Megawatt-Rated Direct AC/AC Power Electronics Converters, IEEE Transactions on Powe Electronics, Vol.30, No. 7, July 2015, pp.3553-3562.

[7] Li H.L., A.Hu, G. Covic, A Direct AC-AC Converter for Inductive Power- Transfer Systems ,IEEE Transactions on Power Electronics, Vol.27, No. 2, February 2012, pp.661-669.

[8] Li H.L., A.Hu, G. Covic Current Fluctuation Analysis of a Quantum ac-ac Resonant Converter for Contactless Power Transfer, Energy Conversion Congress and Symposium Proceedings, 2010, pp.1838-1843.

[9] Sigimura H., S. Mun, S. Kwon, T. Mishima, M. Nakaoka, High Frequency Resonant Matrix Converter using One-Chip Reverse Blocking IGBT-Based Bidirectional Switches for Induction Heating Power Electronics Specialist Conference Proceedings, 2008, pp.3960-3966.

[10] Sornago H., O. Lucia, A. Mediano, J. Burdio, A Class-E Direct AC-AC Converter With Multicicle Modulation for Induction Heating Systems, IEEE Transactions on Industrial Electronics, Vol.61, No.5, May 2014, pp.2521-2531.

[11] Aldhaher S., P. Luk, A. Bati, Wireless Power Transfer Using Class E Inverter with Saturable DC-Feed Inductor, IEEE Transactions on Industry Applications, Vol.50, No.4, 2014, pp.2710-2718.

[12] Kaczmarczyk Z., A high-efficiency Class E inverter – computer model, laboratory measurement and SPICE simulation, Bulletin of the Polish Academy of Sciences, vol.55, No.4, 2007, pp.411-417.